Sensitivity analysis and identification of material defects in dynamical systems

Tadeusz Burczyński, Marc Bonnet, Piotr Fedeliński, Marek Nowakowski

SENSITIVITY ANALYSIS AND IDENTIFICATION OF MATERIAL DEFECTS IN DYNAMICAL SYSTEMS

TADEUSZ BURCZYŃSKI[a]*, MARC BONNET[b], PIOTR FEDELIŃSKI[a] and MAREK NOWAKOWSKI[a]

[a]*Silesian University of Technology, Dept. for Strength of Materials and Computational Mechanics, 18A Konarskiego St., 44-100 Gliwice, Poland;* [b]*CNRS, Laboratoire de Mecanique des Solides, Ecole Polytechnique 91128 Palaiseau Cedex, France*

(Received 23 May 2000)

This paper deals with an analytical and computation strategy, based on the adjoint variable approach and boundary integral equation (BIE) formulations, for evaluating void or crack shape sensitivities of objective functionals. Boundary-only expressions for such sensitivities are sought in the context of linear elastodynamics. An evolutionary hybrid algorithm with the gradient mutation is employed for the identification of material defects. Numerical tests of sensitivity expressions and identification of an internal crack and void are presented.

Keywords: Sensitivity analysis; Adjoint variable approach; Defect identification; Elastodynamics; Crack problem; Boundary element method (BEM); Evolutionary hybrid algorithm

1. INTRODUCTION

The need to compute the sensitivity of integral functionals with respect to shape parameters arises in many situations where a geometrical domain plays the primary role; shape optimization and inverse problems are the most obvious with such instances. In addition to numerical differentiation techniques, shape sensitivity evaluation can be based on either the direct differentiation or the adjoint variable approach. The direct differentiation approach is in particular applicable in the presence of cracks. Following this approach, a shape sensitivity computation relies on solving as many new boundary-value problems as the numbers of shape parameters present [1]. The adjoint variable approach is even more attractive, since it needs to solve only one new initial boundary-value problem (the adjoint problem), whatever be the number of shape parameters. The adjoint variable approach has been successfully applied to many shape sensitivity problems [3]. However, when geometrical domain contains cracks or other geometrical singularities, divergent integrals associated with e.g. crack tip singularity of field variable arise, and obtaining a boundary-only expression raises mathematical difficulties. The present paper deals with the formulation of the adjoint variable method applied to crack shape sensitivity analysis, in connection with the use of boundary integral equation (BIE) formulations for elastodynamics in the time domain. In order to solve the defect identification problem the evolutionary hybrid approach is proposed. This approach is based on a coupling of an evolutionary algorithm and a gradient algorithm. A special gradient mutation is employed, in which shape sensitivity information is used.

2. FORMULATION OF THE PROBLEM

Consider a bounded body B with an external boundary S, containing an internal defect in the form of a void V of boundary Γ (see Fig. 1a) or a crack with crack surface Γ (see Fig. 1b). Let Ω denote the actual body (i.e. containing the defect): $\Omega = B \backslash V$ or $\Omega = B \backslash \Gamma$ and $\partial\Omega = S \cup \Gamma$.

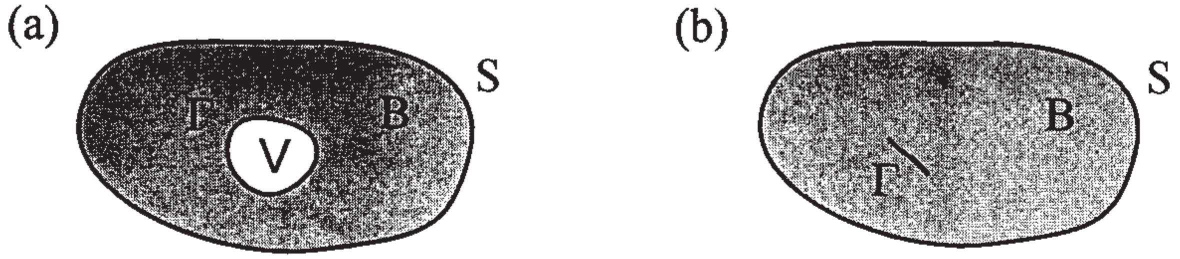

FIGURE 1 A body with an internal defect: (a) a void, (b) a crack.

The displacement $\mathbf{u}$, strain $\boldsymbol{\varepsilon}$ and stress $\boldsymbol{\sigma}$ are related by well-known field equations of linear elastodynamics in the time domain ($\mathbf{C}$: fourth-order elasticity tensor):

$$\operatorname{div}\boldsymbol{\sigma} - \rho\ddot{\mathbf{u}} = 0; \quad \boldsymbol{\sigma} = \mathbf{C} : \boldsymbol{\varepsilon}; \quad \boldsymbol{\varepsilon} = \tfrac{1}{2}(\nabla\mathbf{u} + \nabla^T\mathbf{u}) \quad \text{in}\,\Omega. \tag{1}$$

Equation (1) are completed with boundary and initial conditions. A given traction $\bar{\mathbf{f}}$ is imposed on a part of boundary S, while on the rest of S a displacement $\bar{\mathbf{u}}$ is known. A boundary Γ is traction-free and initial rest is assumed. A traction vector $\mathbf{f} = \boldsymbol{\sigma}\cdot\mathbf{n}$ is defined in terms of the outward unit normal $\mathbf{n}$ to $\partial\Omega$. In the crack case the displacement $\mathbf{u}$ is allowed to jump across Γ; $[\![\mathbf{u}]\!] = \mathbf{u}^+ - \mathbf{u}^- \neq \mathbf{0}$.

A shape and position of the boundary Γ characterizing the defect are unknown. Consider the problem of finding the shape and position of the defect using elastodynamic experimental data, as in ultrasonic measurements. The lack of information about V and Γ is compensated by some knowledge about $\mathbf{u}$ on S (redundant boundary data). Assume that a measurement $\hat{\mathbf{u}}(\mathbf{x}, t)$ of $\mathbf{u}$ is available for $\mathbf{x} \in S_m \subseteq S$ and $t \in [0, T]$. The usual approach for finding Γ consists in the minimization of some distance J between $\mathbf{u}_\Gamma$ (computed) and $\hat{\mathbf{u}}$ (measured), e.g.

$$J(\Gamma) = \int_0^T \int_{S_m} \varphi(\mathbf{u}_\Gamma, t)\,\mathrm{d}S\,\mathrm{d}t; \quad \varphi = \tfrac{1}{2}(\hat{\mathbf{u}} - \mathbf{u}_\Gamma)^2, \tag{2}$$

where $\mathbf{u}_\Gamma$ denotes the solution of the problem (1) for a given location Γ.

The minimization of J with respect to Γ needs in turn, for efficiency, the evaluation of the functional J and its gradient with respect to perturbations of Γ.

3. SHAPE SENSITIVITY ANALYSIS

Consider in the m-dimensional Euclidean space R^m, $m = 2$ or 3, a body Ω_p whose shape depends on a finite number of shape parameters $\mathbf{p} = \{p_1, p_2, \ldots, p_n\}$. Shape parameters are treated as time-like parameters using a continuum kinematics-type Lagrangian description and initial configuration conventionally associated with $\mathbf{p} = \mathbf{0}$

$$\mathbf{x} \in \Omega_0 \to \mathbf{x}^p = \boldsymbol{\Phi}(\mathbf{x},\mathbf{p}) \in \Omega_p \tag{3}$$

with $\Phi(\mathbf{x},0)=\mathbf{x}(\forall \mathbf{x}\in\Omega_0)$. The geometrical transformation $\Phi(\cdot,\mathbf{p})$ must possess a strictly positive Jacobian for any given $\mathbf{p}$. As far as first-order derivatives with respect to $\mathbf{p}$ are concerned, attention can be restricted to the consideration of a single shape parameter p without loss of generality.

The initial transformation velocity field $\boldsymbol{\theta}(\mathbf{x})$, defined by

$$\boldsymbol{\theta}(\mathbf{x})=\frac{\partial\Phi}{\partial\mathbf{p}}(\mathbf{x},p\,=\,0) \tag{4}$$

is the 'initial' velocity of the 'material' point which coincides with the geometrical point $\mathbf{x}$ at time $p=0$. One assumes here that the external boundary S and its neighborhood are unaffected by the shape transformation, so $\boldsymbol{\theta}=\mathbf{0}$ and $\nabla\boldsymbol{\theta}=\mathbf{0}$ on S. However, this is not true in case of an emerging crack. Introduce the following Lagrangian, in which the weak formulation of the direct problem (1) appears as an equality constraint term added to the objective function J:

$$\begin{aligned} L(\mathbf{u},\boldsymbol{v},\Gamma)=J(\mathbf{u},\Gamma)&+\int_0^T\int_\Omega[\boldsymbol{\sigma}(\mathbf{u})\colon\nabla(\boldsymbol{v})+\rho\ddot{\mathrm{u}}\cdot\boldsymbol{v}]\,\mathrm{d}\Omega\,\mathrm{d}t\\ &-\int_0^T\int_s\bar{\mathbf{f}}\cdot\boldsymbol{v}\,\mathrm{d}S\,\mathrm{d}t \end{aligned} \tag{5}$$

where $\boldsymbol{v}$ is a test function. After some transformations one can express the derivative of J as the total material derivative of the Lagrangian with respect to a variation of the domain [2].

$$\begin{aligned} \frac{\mathrm{d}}{\mathrm{d}p}J(\Gamma)=\frac{\mathrm{d}}{\mathrm{d}p}L(\mathbf{u}_\Gamma,\boldsymbol{v}_\Gamma,\Gamma)&=\int_0^T\int_\Omega[\boldsymbol{\sigma}(\mathbf{u})\colon\varepsilon(\boldsymbol{v})+\rho\ddot{\mathbf{u}}.\boldsymbol{v}]\,\mathrm{div}\,\boldsymbol{\theta}\,\mathrm{d}\Omega\mathrm{d}t\\ &-\int_0^T\int_\Omega[\boldsymbol{\sigma}(\mathbf{u}).\nabla(\boldsymbol{v})+\boldsymbol{\sigma}(\boldsymbol{v})\cdot\nabla(\mathbf{u})]\colon\nabla\boldsymbol{\theta}\,\mathrm{d}\Omega\,\mathrm{d}t \end{aligned} \tag{6}$$

Now $\boldsymbol{v}$ is a solution of the adjoint problem, described by Eq. (1) with the following boundary and final conditions:

$$\mathbf{f}(\boldsymbol{v})=-\frac{\partial\varphi}{\partial\mathbf{u}}\quad\text{on } S;\quad \mathbf{f}(\boldsymbol{v})=\mathbf{0}\ \text{ on }\Gamma;\quad \boldsymbol{v}=\dot{\boldsymbol{v}}=\mathbf{0}\quad\text{in }\Omega,\quad\text{at } t=T. \tag{7}$$

The adjoint problem can be solved in the same way as the direct problem, but time-reversed. The expression (6) is valid for any shape transformation and uses the primary and adjoint solution.

4. SHAPE SENSITIVITY: BOUNDARY INTEGRAL FORMULATION FOR THE VOID AND CRACK PROBLEM

The formula (6) for the sensitivity of J is expressed by a domain integral, but it can be converted into an equivalent boundary-only expression in the case of the void problem [2]:

$$\frac{\mathrm{d}J}{\mathrm{d}p} = \int_0^T \int_\Gamma [\boldsymbol{\sigma}(\mathbf{u}) : \nabla(\boldsymbol{v}) - \rho \dot{\mathbf{u}} \cdot \dot{\boldsymbol{v}}]\boldsymbol{\theta} \cdot \mathbf{n} \, \mathrm{d}S \, \mathrm{d}t. \tag{8}$$

Consider the case where unknown defect is a crack, i.e. the limiting case of a void bounded by two surfaces Γ^+ and Γ^- identical and of opposite orientation. It is tempting to still apply Eq. (8) to compute sensitivities with respect to crack location perturbation, but it is not correct. For instance, consider a domain shape transformation such that $\boldsymbol{\theta} = 0$ on the crack surface Γ. This means that crack perturbations along the tangent plane at the crack front are allowed. But then Eq. (8) gives $\mathrm{d}J/\mathrm{d}p = 0$, which is not true. This paradox appears because of the quantity div($\sigma(\mathbf{u})$: $\nabla\boldsymbol{v}$) behaves like d^{-2} in the vicinity of the crack tip (for 2D) and is therefore not integrable (d – distance to the crack tip or front). These difficulties can be overcome by the additive decomposition of the transformation velocity field $\boldsymbol{\theta}$ in the neighborhoods of the crack tips into a constant and a complementary term. Introduce neighborhoods $D_i \subset \Omega$ ($i = 1, 2$) of the two crack tips $\mathbf{x}^i$; the boundary of D_i is denoted by C_i (Fig. 2). Put $\Gamma_i = \Gamma \cap D_i$, $\bar{\Gamma} = \Gamma \backslash (\Gamma_1 \cup \Gamma_2)$ and $\bar{\Omega} = \Omega \backslash (D_1 \cup D_2)$. Then $\partial D_i = C_1 \cup \Gamma_i$ and $\partial\Omega = S \cup C_1 \cup C_2 \cup \bar{\Gamma}$. The transformation velocity field is now expressed

$$\boldsymbol{\mu} = \boldsymbol{\theta} \;\; (\text{in } \bar{\Omega}) \quad \boldsymbol{\mu} = \boldsymbol{\theta} - \boldsymbol{\theta}^i \;\; (\text{in } D_i, i = 1, 2) \tag{9}$$

where $\boldsymbol{\theta}^i = \boldsymbol{\theta}(\mathbf{x}^i)$ is the transformation velocity at the crack tip i.

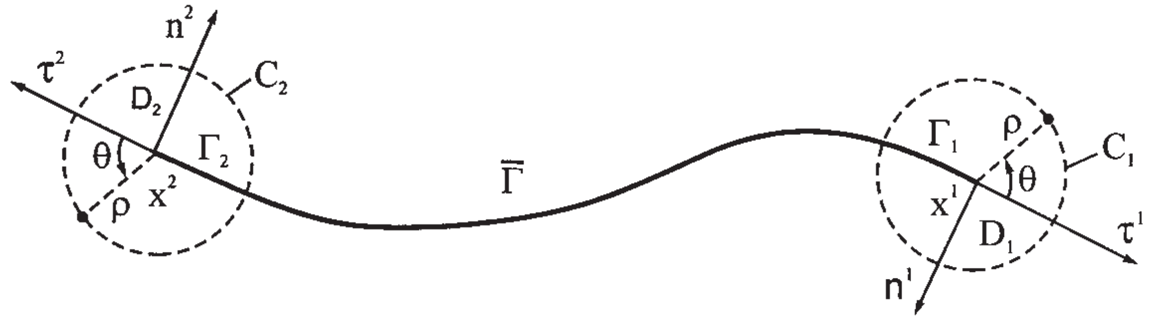

FIGURE 2 Isolation of the crack tips by neighborhoods $D_i\,(i=1{,}2)$; notation.

Now the integration by parts on Eq. (6) is carried out separately in each subdomain $\bar{\Omega}, D_1, D_2$ and with $\boldsymbol{\theta}$ replaced by $\boldsymbol{\mu}$. Keeping in mind that $\boldsymbol{\mu}$ is discontinuous across $\mathbf{C}_i$, one obtains

$$\begin{aligned}\frac{\mathrm{d}}{\mathrm{d}p}J(\Gamma) &= \int_0^T \int_\Gamma [[\boldsymbol{\sigma}(\mathbf{u})\colon \nabla(\boldsymbol{v}) - \rho\dot{\mathbf{u}}\cdot\dot{\boldsymbol{v}}]]\,\boldsymbol{\mu}_n\,\mathrm{d}S\,\mathrm{d}t \\ &\quad - \sum\nolimits_{i=1}^{2} \int_0^T \int_{\mathrm{C}_i} [\boldsymbol{\sigma}(\mathbf{u})\colon \nabla(\boldsymbol{v}) - \rho\dot{\mathbf{u}}\cdot\dot{\boldsymbol{v}}](\boldsymbol{\theta}^i\cdot\mathbf{n})\,\mathrm{d}S\,\mathrm{d}t \\ &\quad + \sum\nolimits_{i=1}^{2} \int_0^T \int_{\mathrm{C}_i} [\mathbf{f}(\boldsymbol{v})\colon \nabla(\boldsymbol{v}) + \mathbf{f}(\mathbf{u})\colon \nabla(\boldsymbol{v})]\,\boldsymbol{\theta}^i\mathrm{d}S\,\mathrm{d}t\end{aligned} \tag{10}$$

where the various normal vectors are as indicated in Fig. 2.

The formula (10) can be expressed also by means of stress intensity factors SIFs [4]. Assume that the dynamical SIFs $\mathrm{K}_{\mathrm{I}}^{u}(t;\mathbf{x}^i), \mathrm{K}_{\mathrm{II}}^{u}(t;\mathbf{x}^i)$, $\mathrm{K}_{\mathrm{I}}^{v}(t;\mathbf{x}^i), \mathrm{K}_{\mathrm{II}}^{v}(t;\mathbf{x}^i)$ at tip $\mathbf{x}^i$, associated with the solutions of the primary and adjoint problems, respectively are known. Since the curves C_i are arbitrary, one may follow the procedure that allows linking J-integral to SIFs, i.e. assume that C_i is the circle of radius $\boldsymbol{\varepsilon}$ centered at crack tip $\mathbf{x}^i$ and investigate the limiting case $\boldsymbol{\varepsilon}\to 0$. In this limit, Eq. (10) is:

$$\begin{aligned}\frac{\mathrm{d}}{\mathrm{d}p}J(\Gamma) &= \int_0^T \int_\Gamma [[\boldsymbol{\sigma}(\mathbf{u}) : \nabla(\boldsymbol{v}) - \rho\dot{\mathbf{u}}\boldsymbol{\cdot}\dot{\boldsymbol{v}}]]\,\boldsymbol{\theta}\boldsymbol{\cdot}\mathbf{n}\,\mathrm{d}S\,\mathrm{d}t - \frac{1-\nu}{\mu} \\ &\quad \times \sum\nolimits_{i=1}^{2} \int_0^T \begin{bmatrix} (\mathrm{K}_{\mathrm{I}}^{u}(t;\mathbf{x}^i)\mathrm{K}_{\mathrm{I}}^{v}(t;\mathbf{x}^i) + \mathrm{K}_{\mathrm{II}}^{u}(t;\mathbf{x}^i)\mathrm{K}_{\mathrm{II}}^{v}(t;\mathbf{x}^i))\,(\theta_\tau^i) \\ -(\mathrm{K}_{\mathrm{I}}^{u}(t;\mathbf{x}^i)\mathrm{K}_{\mathrm{II}}^{v}(t;\mathbf{x}^i) + \mathrm{K}_{\mathrm{II}}^{u}(t;\mathbf{x}^i)\mathrm{K}_{\mathrm{I}}^{v}(t;\mathbf{x}^i))\,(\theta_n^i) \end{bmatrix} \mathrm{d}t\end{aligned} \tag{11}$$

where $\boldsymbol{\theta}_\tau^i, \boldsymbol{\theta}_n^i$ are the tangent and normal components (according to Fig. 2) of the crack tip velocity. Equations (10) and (11) in fact involve a time convolution between direct and adjoint quantities; this is a usual feature of adjoint methods employed for time-dependent problems.

5. IDENTIFICATION METHOD

Here a *hybrid evolutionary* algorithm carries out the identification of an internal defect with a boundary Γ. The hybrid algorithm, which connects evolutionary and gradient algorithms together [5], is considerably more efficient than the genetic algorithm, and its application makes the results more accurate.

The objective function (Eq. 2) is now called a fitness function. The hybrid algorithm minimizes the fitness function with respect to defect shape parameters. A vector chromosome characterizes the solution:

$$\mathbf{p} = \{p_1, p_2, \ldots, p_i, \ldots, p_n\} \tag{12}$$

where $p_i, i = 1,2, \ldots n$ are genes which specify a shape and position of the defect. The genes are real numbers on which constraints are imposed in the form:

$$p_{iL} \leq p_i \leq p_{iR}; \quad i = 1, 2, \ldots, n \tag{13}$$

The evolutionary algorithm starts with an initial generation. This generation consists of N chromosomes generated in a random way. Every gene is taken from the feasible domain. The initial generation is then modified by evolutionary operators: Mutation and crossover. Next stage is an evaluation of the fitness function for every chromosome and the selection is employed. The selection is performed in the form of the ranking selection or the tournament selection [6]. The next generation is created and operators work for this generation and the process is repeated. The algorithm is stopped if a chromosome for which the value of the fitness function is zero has been found. An effectiveness of the evolutionary algorithm depends on its operators, which can be defined in a different way.

The crossover operator swaps some chromosome of the selected parents in order to create offspring. Simple, arithmetical and heuristic crossover operators are used.

Simple crossover: This operator needs two parents and produces offspring. The simple crossover may produce an offspring outside the design space. To avoid this, a parameter $\alpha \in [0, 1]$ is applied. For randomly generated crossing parameter i it works as follows (chromosomes $\mathbf{p}_1$, $\mathbf{p}_2$ are parents in the vector form):

$$\begin{aligned} &\text{parent 1:} \quad \mathbf{p}_1 = \{p_1, p_2, \ldots, p_i, \ldots p_n\} \\ &\text{parent 2:} \quad \mathbf{p}_2 = \{e_1, e_2, \ldots, e_i, \ldots e_n\} \end{aligned} \tag{14}$$

$$\text{offspring 1: } \mathbf{p}'_1 = \{p_1, \ldots, p_i, +\alpha e_{i+1} + (1-\alpha)\, p_{i+1}, \ldots, \alpha e_n + (1-\alpha)\, p_n\} \tag{15}$$

$$\text{offspring 2: } \mathbf{p}'_2 = \{e_1, \ldots, e_i, +\alpha p_{i+1} + (1-\alpha)\, e_{i+1}, \ldots, \alpha p_n + (1-\alpha)\, e_n\} \tag{16}$$

Arithmetical Crossover: This operator produces two offspring, which are a linear combination of two parents

$$\mathbf{p}'_1 = \alpha \mathbf{p}_1 + (1-\alpha)\, \mathbf{p}_2; \quad \mathbf{p}'_2 = \alpha \mathbf{p}_2 + (1-\alpha)\, \mathbf{p}_1 \tag{17}$$

Heuristic Crossover: This operator produces a single offspring from two parents:

$$\mathbf{p}'_3 = r(\mathbf{p}_2 - \mathbf{p}_1) + \mathbf{p}_2 \tag{18}$$

where r is a random value from the range [0, 1] and $J(\mathbf{p}_2) \le J(\mathbf{p}_1)$.

Four kinds of mutation operators: Uniform, boundary, non-uniform and gradient mutation are used:

$$\begin{aligned} \text{before mutation: } \mathbf{p}_1 &= \{p_1, p_2, \ldots, p_i, \ldots, p_n\}; \\ \text{after mutation: } \mathbf{p}'_1 &= \{p_1, p_2, \ldots, p'_i, \ldots, p_n\} \end{aligned} \tag{19}$$

Uniform mutation: Offspring are allowed to move freely within the feasible domain and the gene $\mathbf{p}'_i$ takes any arbitrary value from the range $[p_{iL}, p_{iR}]$.

Boundary mutation: The chromosome can take only boundary values of the design space, $\mathbf{p}'_i = p_{iL}$ or $\mathbf{p}'_i = p_{iR}$.

Non-uniform mutation: This mutation operator depends on generation number t and is employed in order to tune the system

$$\mathbf{p}_i' = \begin{cases} p_i + \Delta(t, p_{iR} - p_i) & \text{if a random digit is 0} \\ p_i - \Delta(t, p_i - p_{iL}) & \text{if a random digit is 1} \end{cases} \tag{20}$$

where the function Δ takes value from the range $[0, e]$.

A special type of mutation, so-called *gradient mutation*, is applied. This mutation is characterized by a full genetic interference, which means a modification of genes making use of information about the fitness function gradient.

Gradient Mutation: This single-argument operator changes any chromosome on the ground of fitness function gradient:

$$\mathbf{p}' = \mathbf{p} + \Delta\mathbf{p} \tag{21}$$

where $\Delta\mathbf{p} = \beta\mathbf{h}$, while β is a coefficient determining a step increment in a search direction $\mathbf{h}$. The search direction $\mathbf{h} = \mathbf{h}(\nabla_p J)$ depends on the fitness function gradient $\nabla_p J$, whose elements are determined by Eq. (8) for the case of the void identification or by Eq. (11) for the case of the crack identification. In the paper the steepest descent method is proposed for evaluation of the direction $\mathbf{h} = -\nabla_p J$.

6. NUMERICAL EXAMPLES

Numerical tests have been carried out for two-dimensional problems with internal defects in the form of voids or cracks. Derivatives of the formulated objective function with respect to defect transformation are calculated in order to demonstrate accuracy of the proposed method of crack and flaw shape sensitivity analysis. An identification procedure of the defect based on evolutionary programming and employed information on the gradient of the objective function is presented.

Example 1

A square plate contains an internal defect in the form of a circle void, as it is shown in Fig. 3. The plate has thickness w. One edge is constrained, while the opposite one is loaded by a harmonic traction

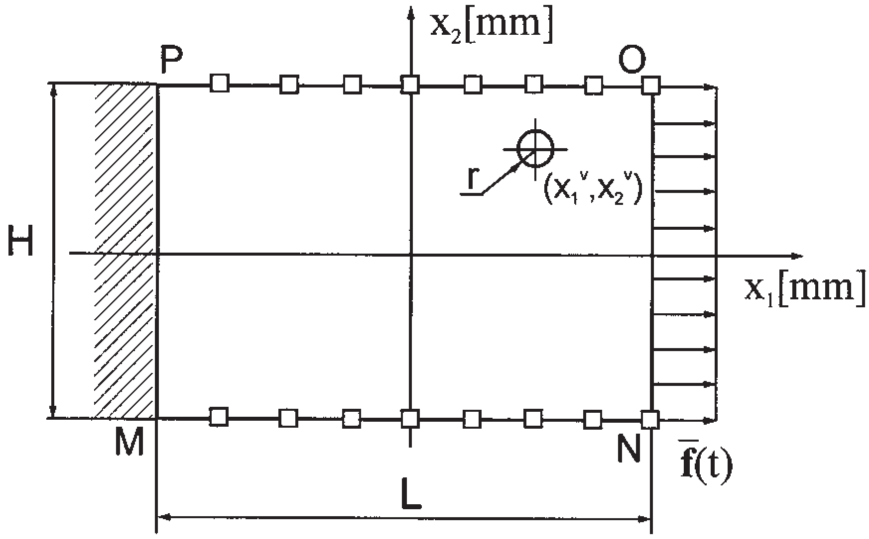

FIGURE 3 The plate with an internal circle defect.

$\bar{\mathbf{f}}(t)$ during the time interval $t \in [0, T]$. Displacements are computed in 32 sensor points located on the boundary S_m. The time step used for the time discretization is Δt. The shape and position of the void is defined by a set of 3 parameters $\mathbf{p} = (x_1^{\nu}, x_2^{\nu}, r)$, which are x_1 and x_2 coordinates of the void center and the void radius, respectively. The plate has the following material properties: The Young modulus $E = 0.2\text{E}12\,\text{Pa}$, the Poisson's ratio $\nu = 0.3$ and the density $\rho = 7800\,\text{kg/m}^3$. The objective function is the following:

$$J(\Gamma) = \int_0^T \int_{S_m} \varphi \, \mathrm{d}S \, \mathrm{d}t \tag{22}$$

where: $\varphi = \frac{1}{2}(\hat{\mathbf{u}}(\mathbf{x}, t) - \mathbf{u}(\mathbf{x}, t))^2$; $\mathbf{x} \in S_m$. The displacement field $\hat{\mathbf{u}}$ is taken from computation for the actual void $\mathbf{p}$.

Sensitivity Analysis

The derivatives of the objective function with respect to transformations of the parameter vector $\mathbf{p}$, are calculated for the void $\mathbf{p}^s$. It needs to solve the primary and the adjoint problems, which are defined in Table I. The derivatives of the objective function (22) are calculated by using Eq. 8. Obtained results are shown in the Table II and compared with a finite difference computation (FD).

Identification of the Void

The identification task is to find the actual void in the plate from Fig. 3, having accurate values of displacements $\hat{\mathbf{u}}(\mathbf{x}, t)$ for $\mathbf{x} \in S_m$ in the time $t \in [0, T]$ and displacements with noise. The noise imposed on the displacements has a Gauss normal distribution with expected value $\hat{\mathbf{u}}(\mathbf{x}, t)$ and standard deviation 1/30 $\hat{\mathbf{u}}(\mathbf{x}, t)$.

The identification process is carried out as minimization of the objective function (22). A minimization method: Hybrid algorithm [5], based on evolutionary and gradient algorithms is used. This method needs value of objective function and its derivative with respect to void transformation.

Figure 4 presents a graph of values of the fitness function for the best chromosome, found in each generation, for the case with and without any noise. The influence of the gradient operator can be seen, which

TABLE I Boundary conditions and geometry of the plate (Fig. 3) for the primary and adjoint problem

Geometry of the plate	$L = H = 200$ mm; $w = 10$ mm Actual void: $\mathbf{p} = \{75, 80, 1\}$ Void for sensitivity: $\mathbf{p}^s = \{74, 79, 1.1\}$ $S_m = \mathrm{MN} \cup \mathrm{OP}$; $S_u = \mathrm{MP}$; $S_p = \mathrm{ON}$
Boundary condition for the primary problem	$\mathbf{f}(t) = \mathbf{f}_0(1 + \sin\omega t)$ on S_p; $\mathbf{f}_0 = 200$ kN/m $\omega = 15708$ rad/s; $T = 800$ μs; $\Delta t = 2$ μs $\mathbf{u}(\mathbf{x}, t) = \mathbf{0}$ on S_u
Boundary condition for the adjoint problem	$\mathbf{f}(t) = \mathbf{u}(\mathbf{x}, \tau) - \hat{\mathbf{u}}(\mathbf{x}, \tau)$; $\tau = T–t$ on S_p

TABLE II Sensitivity results for the void

Case	*Transformation of the void*	dJ/dp	$\Delta J/\Delta p$ *FD*	*Error* $\lvert c–d\rvert/d$ %
a	*b*	*c*	*d*	*e*
(1)	Translation x_1	– 0.7314E–8	– 0.7229E–8	1.2
(2)	Translation x_2	– 0.3049E–7	– 0.3004E–7	1.5
(3)	Expansion	0.2342E–5	0.2306E–5	1.6

TABLE III Void identification results

	$\mathbf{p} = \{x_1^v, x_2^v, r\}$
Actual void	{75.00, 80.00, 1.00}
Solution with no noise	{74.96, 80.04, 0.99}
Solution with the noise	{73.82, 82.13, 0.96}

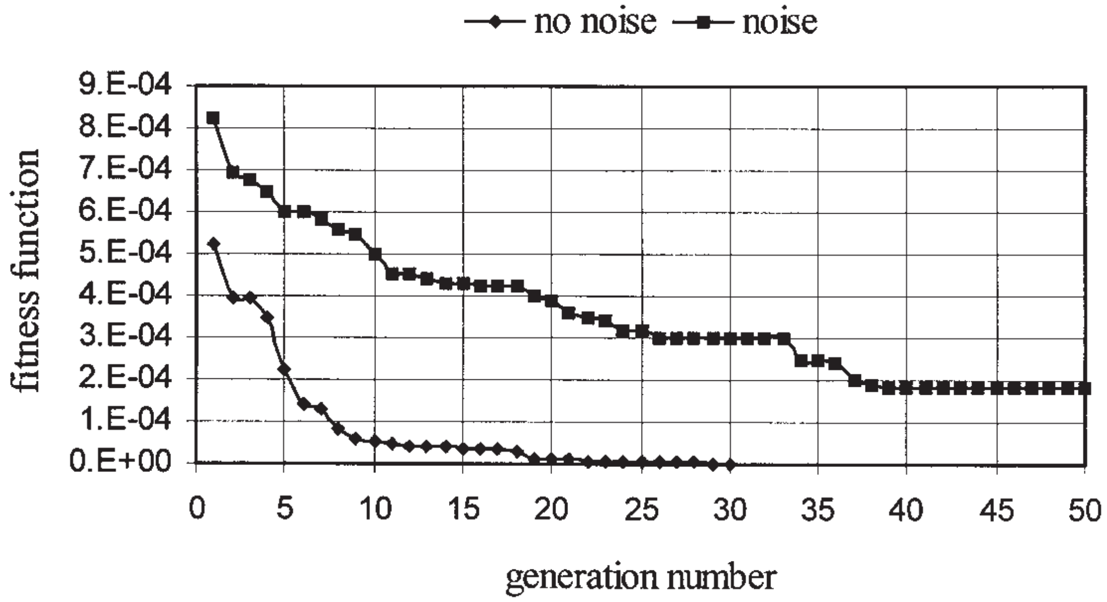

FIGURE 4 Values of the fitness function for the best chromosome in the void identification process

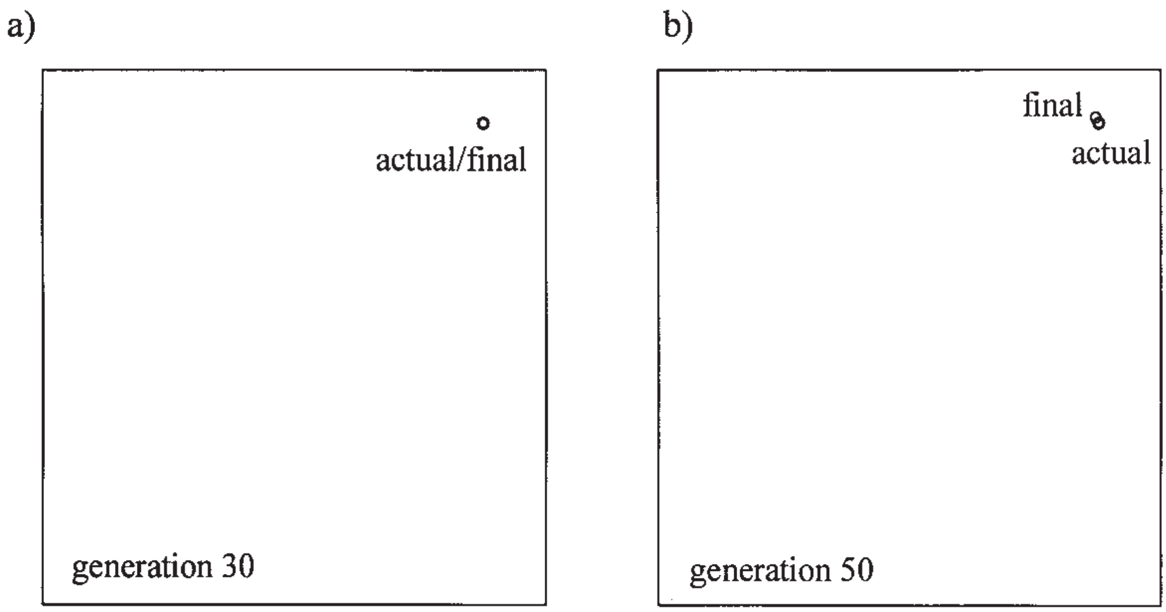

FIGURE 5 Illustration of the void identification process for the case: (a) no noise; (b) noise.

decreases the value of objective function faster than classical genetic algorithm. The identification method works very well for the case without noise (see Fig. 5). When the noise is imposed, the result is less accurate, but still good (see Table III).

Example 2

A square plate contains an internal defect in a form of a straight crack, as it is shown in Fig. 6. The plate has thickness w. One edge is constrained, while the opposite one is loaded by a traction $\bar{\mathbf{f}}(t)$ during the time interval $t \in [0, T]$. Displacements are computed in 32 sensor points located on the boundary S_m. The time step used for the time discretization is Δt. A shape and position of the crack is defined by a set of 4 parameters $\mathbf{p} = \{x_1^c, x_2^c, a, \alpha\}$, which are x_1 and x_2 coordinate of the crack center, length of the crack and angle of the crack respectively. The plate has the same material properties and the objective function as in the Example 1.

Sensitivity Analysis

The derivatives of the objective function with respect to crack shape transformations are calculated for the crack $\mathbf{p}^s$. The primary and the adjoint problem are defined in Table IV. The derivatives of the objec-

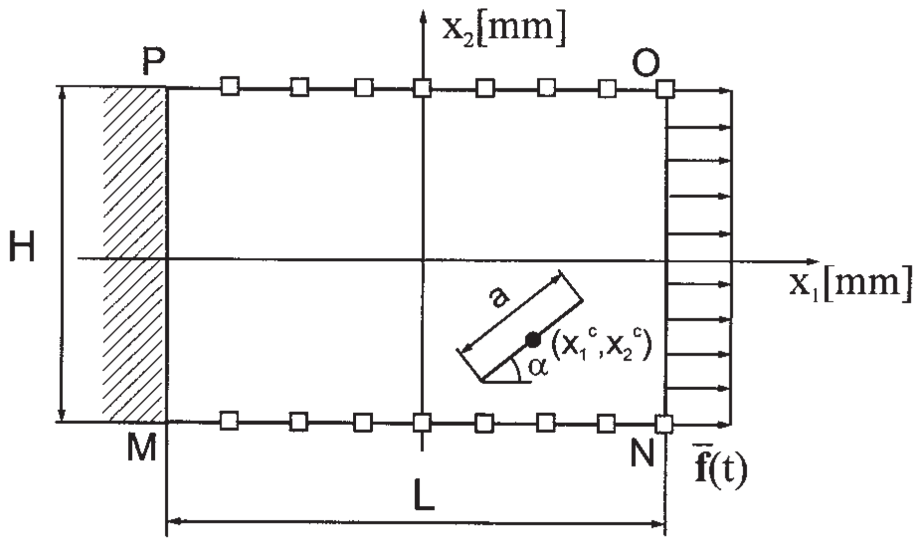

FIGURE 6 The plate with an internal crack.

TABLE IV Boundary conditions and geometry of the plate (Fig. 5) for the primary and adjoint problem

Geometry of the plate	$L = H = 200$ mm; $w = 10$ mm Actual crack: $\mathbf{p} = \{30, -25, 40, 1.18\}$ Crack for sensitivity: $\mathbf{p}^s = \{28, -27, 38, 1.38\}$ $S_m = \mathrm{MN} \cup \mathrm{OP}$; $S_u = \mathrm{MP}$; $S_p = \mathrm{ON}$
Boundary condition for the primary problem	$\mathbf{f}(t) = \mathbf{f}_0 \mathrm{H}(t)$ on S_p $\mathrm{f}_0 = 200$ kN/m; $T = 800\,\mu$s; $\Delta t = 2\,\mu$s $\mathbf{u}(\mathbf{x}, t) = \mathbf{0}$ on S_u
Boundary condition for the adjoint problem	$\mathbf{f}(t) = \mathbf{u}(\mathbf{x}, \tau) - \hat{\mathbf{u}}(\mathbf{x}, \tau)$; $\tau = T - t$ on S_p

tive function (22) are calculated by using Eq. (11). The results are shown in the Table V and compared with a finite difference computation (FD).

Identification of the Crack

The identification task is to find the actual crack in the plate from Fig. 7, having computed displacements $\hat{\mathbf{u}}(\mathbf{x}, t)$ and displacements with a noise. The noise is defined as in Example 1. The identification process is carried out in the same way as for the void in Example 1. An identified crack for the cases: without any noise and with the noise are presented in the Table VI and graphically in Fig. 7. The result for the noise is less accurate, but the information is still useful from the engineering point of view. The history of the identification is shown in Figure 8, in the form of a value of the objective function for the best chromosome in each generation converges very quickly. It demonstrates the efficiency of the identification method.

TABLE V Sensitivity results for the crack

Case *a*	*Transformation of the crack* *b*	$\mathrm{d}J/\mathrm{d}p$ *c*	$\Delta J/\Delta p$ *FD* *d*	*Error* $\lvert c–d\rvert/d$ % *e*
(1)	Translation x_1	−0.9164E−04	−0.9103E−04	0.7
(2)	Translation x_2	−0.5782E−04	−0.5740E−04	0.2
(3)	Expansion	0.2780E−03	0.2727E−03	1.9
(4)	Rotation	0.4672E−03	0.4598E−03	1.6

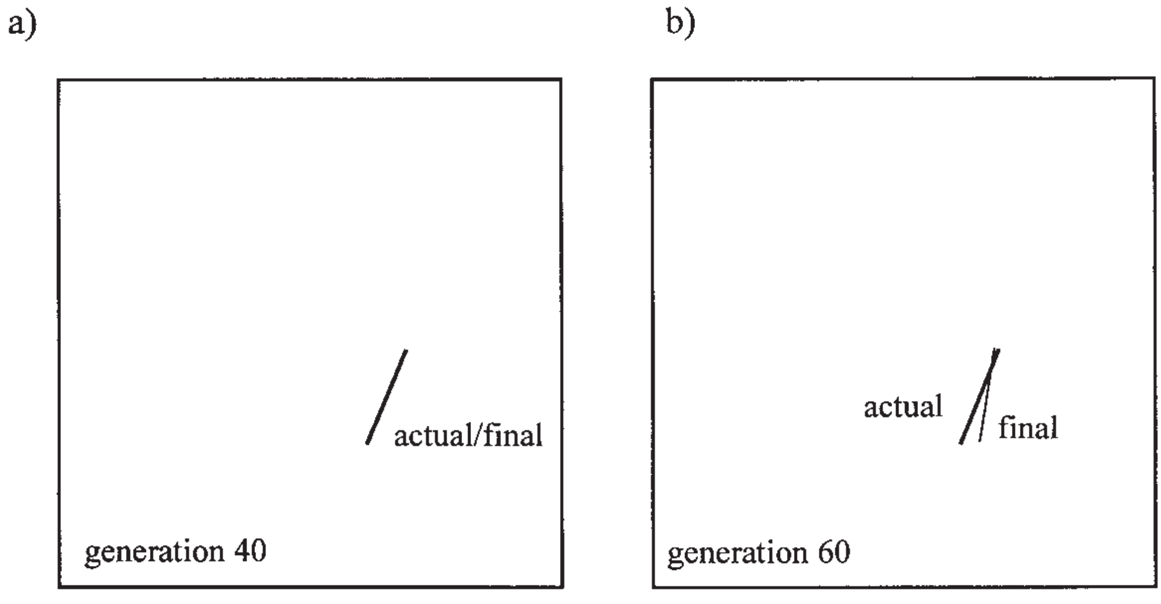

FIGURE 7 Illustration of the crack identification results for the case (a) no noise; (b) noise.

TABLE VI Crack identification results

	$\mathbf{p} = \{x_1^\nu, x_2^\nu, a, \alpha\}$
Actual crack	$\{30.00, -25.00, 40.00, 1.18\}$
Solution with no noise	$\{29.32, -24.56, 39.63, 1.20\}$
Solution with the noise	$\{33.04, -23.57, 38.87, 1.41\}$

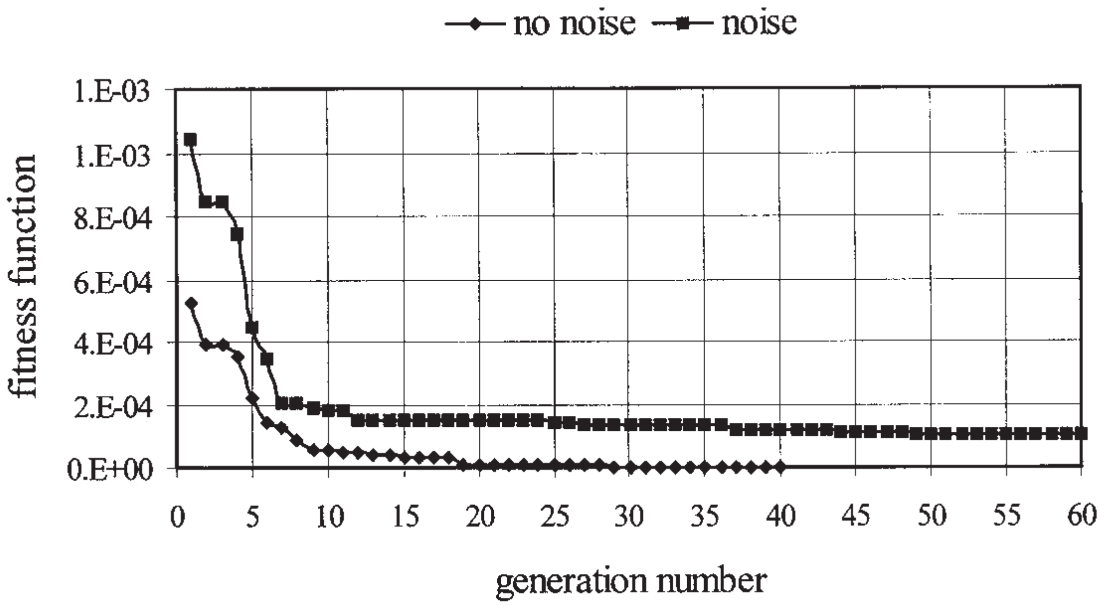

FIGURE 8 Values of the fitness function for the best chromosome in the crack identification process

7. CONCLUDING REMARKS

In the present work a shape sensitivity analysis for identification of internal defects was presented. The main motivation of this paper was to explore the adjoint variable approach, in the presence of cracks and in connection with BIE formulations of the direct problem. The corresponding boundary-only formula for the shape sensitivity of the functional was first established for the case of a void. It was then shown to become inconsistent in the limit when the void became a crack because of the divergence of a certain domain integral. However, resting on the analysis made for the case of a void, functional shape sensitivity expressions which are consistent with the use of BIE formulations and applicable to crack identifications problems were derived. A sensitivity formula involving integrals on the crack and on arbitrary contours around the crack tips was established for 2D situations. It holds regardless of the crack shape and of the shape transformation. Numerical implementation of the analytical expressions for sensitivities has been performed. Numerical tests show, that derivatives of the objective function with respect to defect transformations are in a good agreement with the finite difference method and require less computing time. The evolutionary hybrid algorithm based on the gradient mutation is employed for identification of voids and cracks. The presented results are very accurate for the defect identification in the absence of noise. Even if noise is added in the objective function, the results remain reasonably accurate. This algorithm is considerably more efficient than the genetic algorithm and its application makes the results more accurate.

Acknowledgements

The support from the KBN: grants no. 7 T07A 022 16 and 8 T11F 003 16 is gratefully acknowledged.

References

[1] M. Bonnet (1995). Regularized BIE formulations for first- and second-order shape sensitivity of elastic fields, *Computers and Structures*, **56**, 799–811.

[2] M. Bonnet, T. Burczyński and M. Nowakowski (June 13, 1999). A BEM– and adjoint, variable-based approach to crack shape sensitivity analysis, *Proceedings of IPE*, Port Ludlow, USA.

[3] T. Burczyński (1993). Application of BEM in sensitivity analysis and optimization, *Comp. Mech.*, **13**, 29–44.

[4] P. Fedeliński, M.H. Aliabadi and D.P. Rooke (1996). Boundary element formulations for the dynamic analysis of cracked structures, *Engen. Anal. with Bound. Elem.*, **17**, 45–56.

[5] T. Burczyński and P. Orantek (1999). Coupling of genetic and gradient algorithms, *Proc. 3rd Conference of Evolutionary Algorithms and Global Optimization*, Złoty Potok.

[6] Z. Michalewicz (1992). *Genetic Algorithms + Data Structures = Evolutionary Programs*, Springer-Verlag, AI Series, New York.